Enhanced Time Division Duplexing Slot Allocation and Scheduling in Non-Terrestrial Networks

Alessandro Traspadini, Marco Giordani, Michele Zorzi

Department of Information Engineering, University of Padova, Italy. Email: {traspadini, giordani, zorzi}@dei.unipd.it

Abstract—The integration of non-terrestrial networks (NTNs) and terrestrial networks (TNs) is fundamental for extending connectivity to rural and underserved areas that lack coverage from traditional cellular infrastructure. However, this integration presents several challenges. For instance, TNs mainly operate in Time Division Duplexing (TDD). However, for NTN via satellites, TDD is complicated due to synchronization problems in large cells, and the significant impact of guard periods and long propagation delays. In this paper, we propose a novel slot allocation mechanism to enable TDD in NTN. This approach permits to allocate additional transmissions during the guard period between a downlink slot and the corresponding uplink slot to reduce the overhead, provided that they do not interfere with other concurrent transmissions. Moreover, we propose two scheduling methods to select the users that transmit based on considerations related to the Signal-to-Noise Ratio (SNR) or the propagation delay. Simulations demonstrate that our proposal can increase the network capacity compared to a benchmark scheme that does not schedule transmissions in guard periods.

Index Terms—Non-terrestrial networks (NTNs); Satellite communication; Time Division Duplexing (TDD); Scheduling.

I. INTRODUCTION

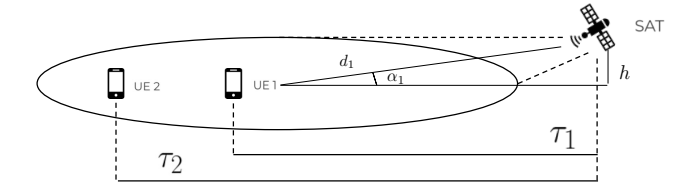
The research community is studying non-terrestrial networks (NTNs) as an approach to extend ground coverage in extreme environments, such as in remote or unconnected areas [1], and provide connectivity in case of emergency [2]. Notably, the integration and coordination between NTNs and terrestrial networks (TNs) is particularly promising to improve service continuity, availability, and scalability [3].

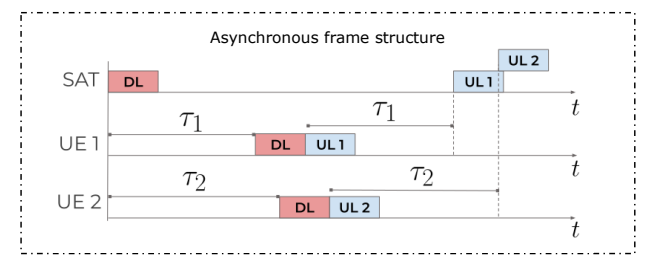
In this context, the 3rd Generation Partnership Project (3GPP) has consolidated the possible use of satellites, especially Low Earth Orbit (LEO) satellites, into the 5G New Radio (NR) cellular standard since Release 15 [4], [5], and a new Work Item on 3GPP NTN has been officially approved in Release 17 [6]. Direct-to-handset satellite communication for unmodified smartphones is also being promoted. However, to date, the 3GPP NTN standard has not yet been fully formalized, also with respect to the baseline 5G NR terrestrial protocol stack. The key challenges include the longer propagation delay and more severe propagation loss of the satellite channel with respect to TNs, and the large Doppler shifts and velocity of satellite platforms [7], [8]. Several studies have proposed solutions to address these problems. For instance, Han *et al.* proposed to relocate the functions of mobility

management to satellites to improve flexibility and reduce delays [9]. Similarly, Peng *et al.* investigated interference mitigation techniques to facilitate the integration of multibeam satellite systems with TNs [10]. The analysis on co-channel interference in integrated TN/NTN systems was further discussed in [11], [12]. Additionally, Zu *et al.* presented a cooperative transmission design for TN/NTN systems with the objective of improving coverage and capacity [13].

To date, a major compatibility issue between TNs and NTNs is related to the duplex communication. In fact, most satellite networks are designed in Frequency Division Duplexing (FDD) [14]. In FDD, User Equipments (UEs) and satellites operate on different frequency bands for uplink (UL) and downlink (DL) slots. This approach permits full-duplex communication via simultaneous and continuous UL and DL transmissions, eliminates the need for tight synchronization, and promotes interference mitigation as UEs communicate in orthogonal frequency bands. In turn, terrestrial 5G NR networks operate in Time Division Duplexing (TDD) [15]. The advantages include channel reciprocity, dynamic and flexible traffic allocation, lower hardware costs, and frequency diversity [16]. However, to guarantee full and seamleass integration between TNs and NTNs, the 3GPP suggests that NTNs be designed also in TDD [4], which may raise several concerns. First, the length of guard periods, which ensure that consecutive UL and DL transmissions do not interfere, must be proportional to the cell size and propagation delay. Both are particularly large in satellite networks, and may span several transmission slots, with negative implications in terms of overhead. Second, TDD requires synchronization, which is difficult in satellite networks due to differential delays that could be experienced by two or more UEs within the same cell, especially at low elevation. In 3GPP, Timing Advance (TA) was introduced to compensate for the propagation delays between UEs and the satellite to achieve synchronization. Still, this approach prevents the network from scheduling TDD transmissions during guard periods to avoid interference, which results in large overheads and inefficient use of resources.

To address these issues, in this paper we propose a novel slot allocation mechanism, called Enhanced Synchronized Slot Allocation (ESSA), to improve capacity in TDD NTN. Specifically, the idea is to reduce the number of guard periods, where transmissions may not be formally scheduled,





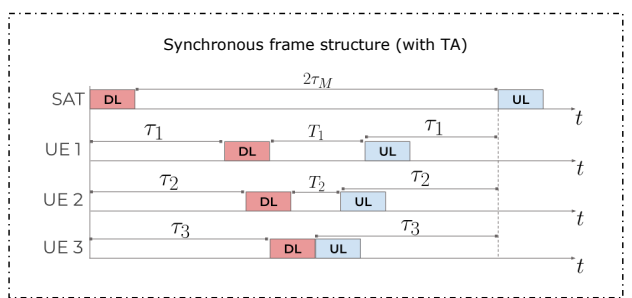


Fig. 1: Illustration of the scenario for $N_{\rm UE}=2$ (top), and the TDD frame structure with (middle) and without (bottom) timing advance.

by allocating multiple (rather than just one) DL slots before a UL slot, if these transmissions do not generate interference at the satellite. Moreover, we propose two scheduling methods to select the optimal UEs that should transmit in TDD to maximize the network capacity. Scheduling is based on either the best link quality (MG) or the minimum differential delay (MS). We evaluate the performance of ESSA, as well as of MG and MS, against a TDD benchmark scheme that does not schedule additional transmissions during guard periods, but only implements TA for synchronization. We demonstrate via simulations that ESSA can increase the channel usage by nearly 50%, and that the capacity of MS combined with ESSA is around three times higher than that of MG with TA.

The remainder of this paper is structured as follows. In Sec. II we present the system model, in Sec. III we introduce ESSA and the proposed scheduling methods, in Sec. IV we describe our simulation results, and in Sec. V we conclude the paper with suggestions for future work.

II. SYSTEM MODEL

Our NTN scenario, depicted in Fig. 1 (top), consists of $N_{\rm UE}$ UEs that are connected through direct-to-satellite links to a single LEO satellite (SAT) providing Next Generation Node Base (gNB) functionalities at an altitude h. The system is assumed to be steady, with fixed propagation delays for both UL and DL transmissions, as the mobility of the satellite on its orbit and that of the UEs can be neglected at the subframe

level. As described in [17], the distance d_i from the satellite to a generic UE i is given by

$$d_i = \sqrt{R_E^2 \sin^2(\alpha_i) + h^2 + 2hR_E} - R_E \sin(\alpha_i),$$
 (1)

where R_E is the Earth's radius, and α_i is the elevation angle between UE i and the satellite. In the following, we describe the channel model (Sec. II-A) and the TDD frame structure (Sec. II-B).

A. Channel Model

In this study we consider the 3GPP NTN channel model with shadowing in an urban scenario [4]. The path loss between the satellite and UE i is given by:

$$PL_i = FPL_i + A_a + A_s + SF \tag{2}$$

where FPL is the free-space path loss (FSPL), A_g is the atmospheric absorption loss due to dry air and water vapor attenuation, and A_s is the scintillation loss due to sudden changes in the refractive index caused by variations of the temperature, water vapor content, and barometric pressure [19]. SF represents the shadowing component, which is modeled as a zero mean log-normal random variable with variance σ_s . The value of σ_s depends on various factors including channel conditions, the scenario, and the elevation angle, as described in [4]. The FSPL is given by:

$$FPL_i = 92.45 + 20\log_{10}(f) + 20\log_{10}(d_i), \tag{3}$$

where f represents the carrier frequency in GHz and d_i is the distance in kilometers. The received power P_i^{rx} of UE i is expressed as

$$P_i^{rx} = P^{tx} + G^{tx} + G^{rx} - PL_i, (4)$$

where P^{tx} is the transmitted power, G^{tx} is the transmitter antenna gain, and G^{rx} is the receiver antenna gain. Thus, the Signal-to-Noise Ratio (SNR) for UE i is given by

$$\gamma_i = P_i^{rx} - 10\log_{10}(kTB) - N_f, \tag{5}$$

where k is the Boltzmann constant, T is the antenna noise temperature, B is the bandwidth, and N_f is the noise figure. From the SNR, the Ergodic capacity C_i of UE i is defined as

$$C_i = B \log_2 \left(1 + 10^{\gamma_i/10} \right).$$
 (6)

B. TDD Frame Structure

The one-way propagation delay for UE i is given by

$$\tau_i = d_i/c,\tag{7}$$

where c is the speed of light. In Fig. 1 (middle) we illustrate the slot allocation in TDD for two UEs under the coverage of the same satellite gNB. The satellite transmits a DL slot, which is received by UE 1 after τ_1 , and by UE 2 after $\tau_2 \gg$

¹A complete characterization of the 3GPP NTN channel model in [4] is described in [18], and implemented in ns-3 here: https://gitlab.com/mattiasandri/ns-3-ntn/-/tree/ntn-dev.

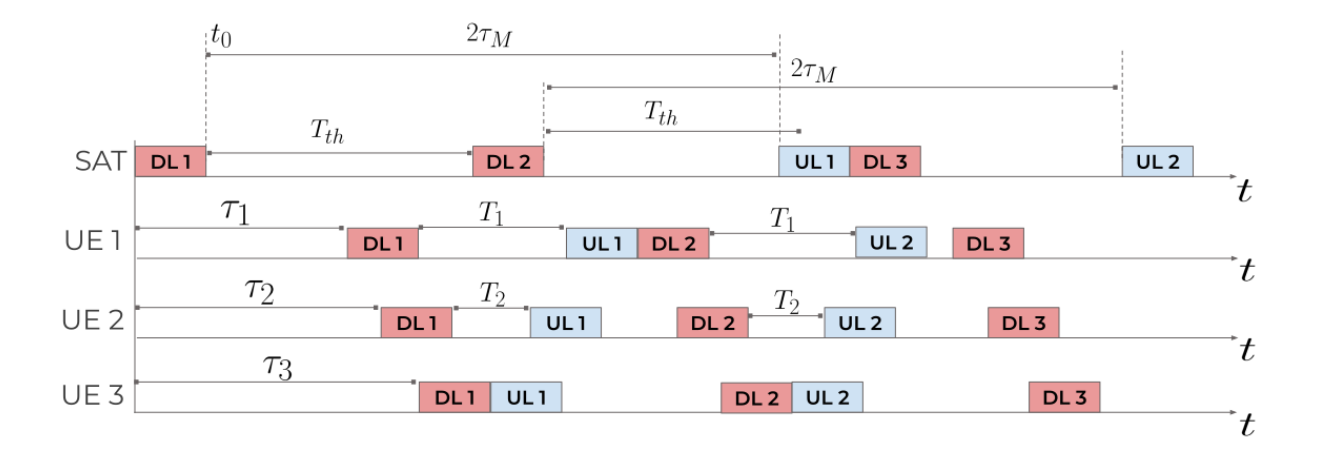


Fig. 2: Illustration of the proposed Enhanced Synchronized Slot Allocation (ESSA) mechanism.

 ${\tau_1.}^2$ If a UL slot for both UEs is allocated immediately after the corresponding DL slot, synchronization of the UL slots at the satellite reference point is not achieved due to the different propagation delays of the UEs. This misalignment results in uncoordinated transmissions, causing interference.

To address this issue, a TA mechanism should be applied [20], [21]. In 3GPP Release 17, each UE is assumed to have knowledge of both its own position and the satellite position using Global Navigation Satellite System (GNSS) coordinates, which permits to estimate the propagation delay of the UL channel [22]. UEs can then report this estimate to the satellite, which computes the longest propagation delay in the cell, denoted as τ_M , corresponding to the furthest UE within the coverage area of the satellite. This information is included in the Physical Downlink Control Channel (PDCCH) to perform TA and maintain synchronization. As shown in Fig. 1 (bottom), if each UE i applies TA of duration $T_i = 2(\tau_M - \tau_i)$, i.e., UL slots are "advanced" by T_i relative to the corresponding DL slots, then UL slots are also synchronized at the satellite reference point. In addition, the satellite can schedule different Orthogonal Frequency Division Multiplexing (OFDM) symbols within the same UL slot to different UEs, without causing interference.

However, in this setup, the guard period between a DL and an UL slot must be equal to $2\tau_M$, thus the overhead depends on the longest link in the network. For a LEO satellite at an altitude of 800 km and with an elevation angle of 70° , the distance at the cell edge, from Eq. (1), is approximately 845 km, resulting in a propagation delay of 2.82 ms. As a result, the guard period is up to 5.64 ms, which is more than the duration of 5 subframes in 5G NR.

The excessive length of guard periods, where no transmissions should be scheduled to avoid interference, would lead to a very inefficient use of radio resources in satellite networks, which motivates our research toward more advanced slot allocation mechanisms, as described in Sec. III.

III. ENHANCED SYNCHRONIZED SLOT ALLOCATION AND SCHEDULING

A. Enhanced Synchronized Slot Allocation (ESSA)

One possible way to reduce the impact of the overhead in TDD is to allocate multiple slots of the same type (i.e., UL or DL), to reduce the number of required guard periods where no transmissions should be scheduled.

Along these lines, in this paper we propose Enhanced Synchronized Slot Allocation (ESSA), which is designed to allocate multiple DL slots during guard periods, before the corresponding UL slot, if they do not interfere with other concurrent transmissions. Let τ_m be the propagation delay of the shortest link in the network, while $t_{\rm UL}$ is the duration of UL transmissions. Then, we define T_{th} as

$$T_{th} = 2(\tau_M - \tau_m) + t_{UL}.$$
 (8)

Lemma 1. In TDD, if a DL transmission is completed at time t_0 , additional concurrent DL transmissions scheduled by the satellite between $t_0 + T_{th}$ and $t_0 + 2\tau_M$ do not create interference, and can be successfully received by all UEs within the coverage area of the satellite.

Proof. Assume that an additional DL slot (DL 2 in Fig. 2), scheduled after T_{th} from the first DL slot (DL 1 in Fig. 2), is received by UE i after $T_{th} + \tau_i$. Moreover, assume that the UL slot relative to the first DL slot (UL 1 in Fig. 2) is transmitted by UE i at $t_0 + \tau_i + 2(\tau_M - \tau_i)$, for a duration of $t_{\rm UL}$. Therefore, the additional DL slot does not interfere if

$$2(\tau_M - \tau_m) + t_{\text{UL}} + \tau_i \ge \tau_i + 2(\tau_M - \tau_i) + t_{\text{UL}},$$
 (9)

which is always verified if $\tau_m \leq \tau_i \ \forall i$, which is true since $\tau_m = \min_i(\tau_i)$.

Indeed, additional DL slots can be scheduled after a time interval equal to $2(\tau_M - \tau_m) + t_{\rm UL}$ from the end of the previous DL slot, provided that $2\tau_m \geq t_{\rm UL}$. This inequality is generally verified in NTN scenarios. For example, for a LEO satellite at an altitude of 600 km, the minimum one-way propagation delay (at the zenith) is approximately $\tau_m = 2$ ms. As a result,

²For a cell radius of 1000 km, the differential propagation delay of UEs in the cell can be up to 10 ms [5, Table 7.2.1.1.1.2-1].

the condition is satisfied if the duration of UL transmissions is $t_{\rm UL} \leq 4$ ms, corresponding to 4 subframes in 5G NR, which is a reasonable assumption in most network configurations. This approach permits to schedule resources that would otherwise be unused because of guard periods, thereby reducing the communication overhead.

As shown in Fig. 2, the second DL slot (DL 2) schedules another UL slot after $2\tau_M$. If there are available slots after a time interval equal to T_{th} from the end of DL 2, other DL slots can be scheduled. For instance, DL 3 is scheduled immediately after the reception of UL 1. This scheduling process continues iteratively until all packets are scheduled. This approach, however, would inevitably reduce the UL capacity in favor of the DL capacity since a lower number of UL slots can be allocated, as we will evaluate in Sec. IV.

B. Scheduling

In order to validate the performance of ESSA, we introduce two scheduling methods that select a subset of $N_s \leq N_{\rm UE}$ UEs that should transmit to maximize the Ergodic capacity of the cell. We call S the set of selected UEs and U the set of available UEs. We consider the following scheduling methods.

• MG (Benchmark): The satellite selects the N_s UEs with the highest SNR, i.e.,

$$S = \underset{S}{\operatorname{arg\,max}} \qquad (\gamma_S) \tag{10a}$$

$$S = \underset{S}{\operatorname{arg\,max}}$$
 (γ_S) (10a)
subject to $\gamma_S = \underset{i \in S}{\min}(\gamma_i),$ (10b)

$$|S| = N_s, (10c)$$

$$S \subseteq U$$
. (10d)

Therefore, MG selects UEs with the best channel conditions in an attempt to maximize the network capacity.

MS: The satellite selects the N_s UEs with the minimum differential propagation delay, i.e.,

$$S = \underset{S}{\operatorname{arg\,min}} \qquad (\tau_S) \tag{11a}$$

$$S = \underset{S}{\operatorname{arg\,min}}$$
 (τ_S) (11a)
subject to $\tau_S = \underset{i,j \in S}{\max} |\tau_i - \tau_j|,$ (11b)

$$|S| = N_s, (11c)$$

$$S \subset U$$
. (11d)

Therefore, MS prioritizes UEs with similar propagation delays, regardless of the actual channel conditions.

These scheduling methods can be combined with ESSA for allocating resources in TDD, as we will demonstrate and evaluate in Sec. IV-B.

IV. SIMULATION RESULTS

The simulation parameters are reported in Table I. Specifically, our scenario consists of a LEO satellite at a fixed altitude $h \in \{300, \dots, 800\}$ km, while the elevation angle α_i of a generic UE i is modeled according to a uniform distribution in $[\alpha_{min}, \alpha_{max}]$, where α_{min} and α_{max} represent the minimum and maximum elevation angles, respectively. We consider UL and DL transmissions in the Ka-bands, i.e., in the millimeter

TABLE I: Simulation parameters.

Parameter	Values
Transmit power (P^{tx}) [dBW]	-6
Total antenna gain $(G^{tx} + G^{rx})$ [dBi]	24
Bandwidth (B) [MHz]	200
Carrier frequency (f) [GHz]	28
Noise temperature (T) [K]	290
Noise figure (N_f) [dB]	5
Number of UEs $(N_{\rm UE})$	100
Selectable UEs (N_s)	10
Maximum elevation angle (α_{max}) [deg]	90
Radius of the Earth (R_E) [km]	6371
Channel parameters $(\{A_g, A_s, \sigma_s\})$	[4]

wave (mmWave) spectrum [23], at frequency f = 28 GHz and with a bandwidth B = 200 MHz.

Results are given in terms of the following metrics:

- Average guard period ($\bar{t}_{\rm GP}$), i.e., the average time between a DL slot and the corresponding UL slot, observed from the satellite reference point.
- Average channel usage $(\bar{\rho})$, i.e., the average percentage of allocated slots (for either UL or DL transmissions) over the total number of available slots. Therefore, it is an indication of the system's overhead. For instance, if $\rho = 0.5$, half of the slots are allocated for transmissions, while the rest is used as guard periods.
- Average capacity (\bar{C}) , i.e., the average of the Ergodic capacity of the N_s selected UEs in the cell via MS or MG scheduling, where the Ergodic capacity of the single UE was defined in Eq. (6).

In Sec. IV-A we will compare the performance of the baseline TDD slot allocation with TA described in Sec. II-B, vs. the proposed ESSA scheme described in Sec. III-A where slot allocation is optimized for NTN. Then, in Sec. IV-B we will compare MG and MS in terms of scheduling.

A. Slot Allocation Results

In this section we compare the performance of TA vs. ESSA in terms of the duration of guard periods and the channel usage. In TA, the guard period is constant and equal to $2\tau_M$, which is required to maintain synchronization via timing advance. In ESSA, additional DL slots can be scheduled during guard periods based on Lemma 1.

Minimum elevation angle: First, in Figs. 3a and 3b we analyze the impact of the minimum elevation angle α_{min} with a LEO satellite at an altitude h = 600 km.³ In general, as $lpha_{min}$ increases, $ar{t}_{\mathrm{GP}}$ decreases. This occurs for TA because the length of the longest link in the network decreases as α_{min} increases, and so does the corresponding propagation delay τ_M . A similar trend is observed for ESSA, as T_{th} also decreases as α_{min} increases. In any case, ESSA outperforms TA. For TA, even with $\alpha_{min} = 70^{\circ}$, which guarantees a good alignment between the LEO satellite and the UEs on the ground, $\bar{t}_{\rm GP} \simeq 4$ ms, with $\bar{\rho} \simeq 5.6\%$.

 3 We investigate the value of α_{min} in the range from 40° to 70° , which is in line with most commercial satellite constellations, as described in [24].

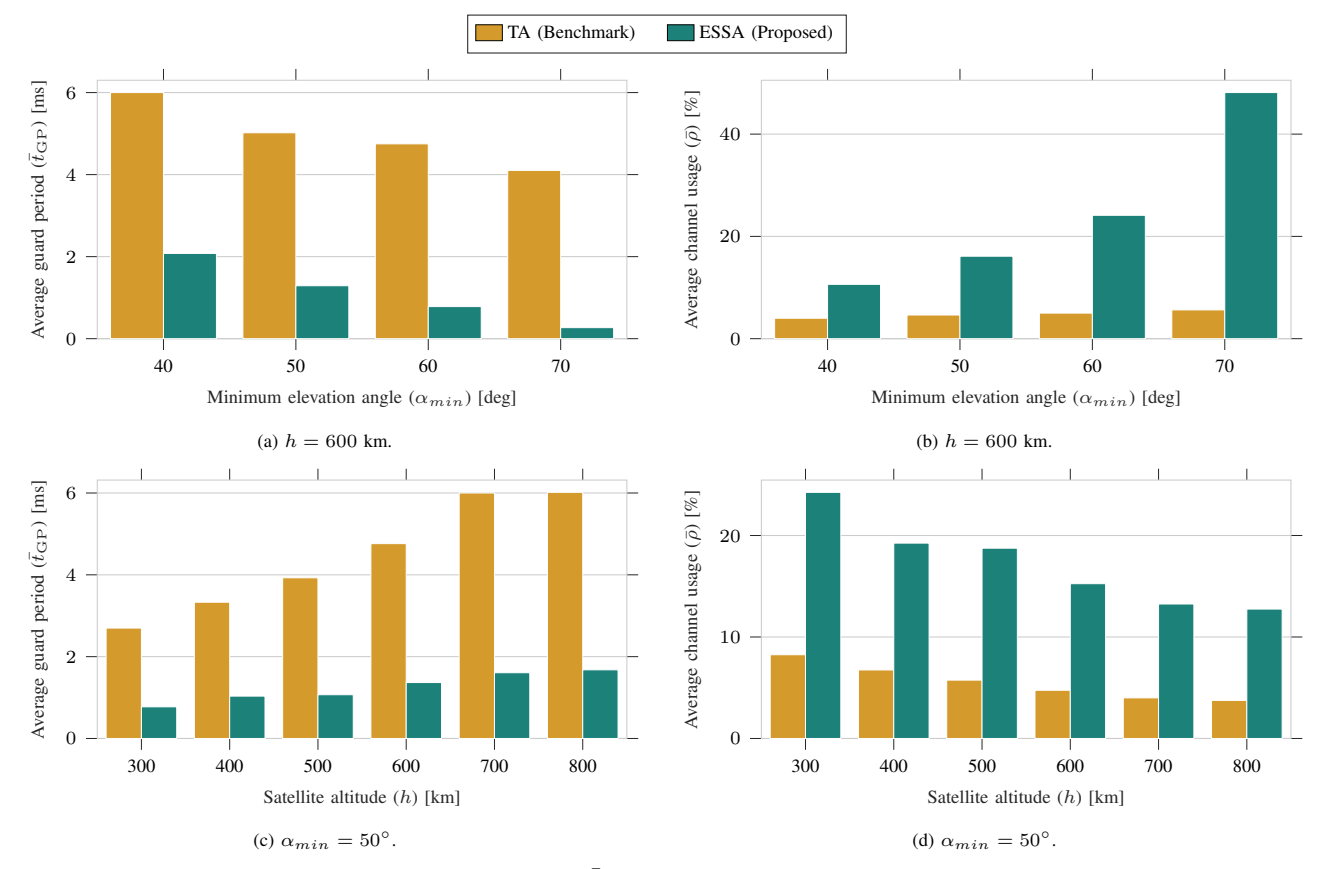


Fig. 3: Average guard period $(\bar{t}_{\rm GP})$ and channel usage $(\bar{\rho})$ vs. α_{min} and h.

In contrast, for ESSA we have $\bar{t}_{\rm GP} < 1$ ms, and $\bar{\rho} \simeq 48\%$. This is because ESSA can schedule multiple DL slots during guard periods before a UL slot, which permits a more efficient use of resources.

Satellite altitude: In Figs. 3c and 3d we analyze the impact of the satellite altitude h, with $\alpha_{min}=50^\circ$. As h increases, both τ_M and T_{th} increase, resulting in a longer guard period for both schemes. At h=300 km, ESSA achieves a channel usage of nearly 25%, with an average guard period of less than 1 ms. Even at h=800 km, ESSA maintains a channel usage of over 10%, i.e., almost three times higher than TA, with a guard period under 2 ms.

The above results demonstrate that ESSA can effectively reduce the overhead for slot allocation compared to TA even in those scenarios characterized by a very long propagation delay, and stands out as a promising approach for NTN.

B. Scheduling Results

We now integrate the two slot allocation schemes presented in Sec. II-B and Sec. III-A (TA and ESSA) with the two scheduling methods presented in Sec. III-B (MG and MS). This results in the following combinations:

 MG-TA and MS-TA: Slot allocation is based on the benchmark TDD frame structure with TA, i.e., with no optimization of guard periods. • MG-ESSA and MS-ESSA: Slot allocation is based on ESSA, so additional DL slots can be allocated during guard periods if $2\tau_m \ge t_{\rm UL}$.

Satellite altitude: First, we explore the impact of h. In Fig. 4a we observe that the path loss increases with h, so the SNR decreases as h increases. For instance, at h=300 km, the median SNR with MG scheduling is approximately 29 dB, vs. 23 dB with MS scheduling. This gap is because MS is based on the propagation delay alone, with no considerations related to the channel quality.

In Fig. 4b we plot the average capacity of the selected N_s UEs via MS or MG scheduling vs. h, considering both TA and ESSA for slot allocation. We see that MS-ESSA outperforms MG-ESSA. In fact, MS is specifically optimized for ESSA. In this scenario, additional DL slots can be allocated if $2\tau_m \geq t_{\rm UL}$: MS prioritizes UEs with the lowest differential propagation delays based on Eq. (11) in an attempt to reduce τ_m and schedule more transmissions, which permits to improve the network capacity. At the same time, MG-TA outperforms MS-TA since MG is explicitly designed to maximize the number of bits per slot and so the capacity. Between the two best configurations, MS-ESSA achieves more than three times the capacity of MG-TA, despite the lower SNR of MS compared to MG. This is because MG-TA is affected by the limitations of TA in terms of overhead and channel usage. In turn, MS-ESSA can scheduled additional

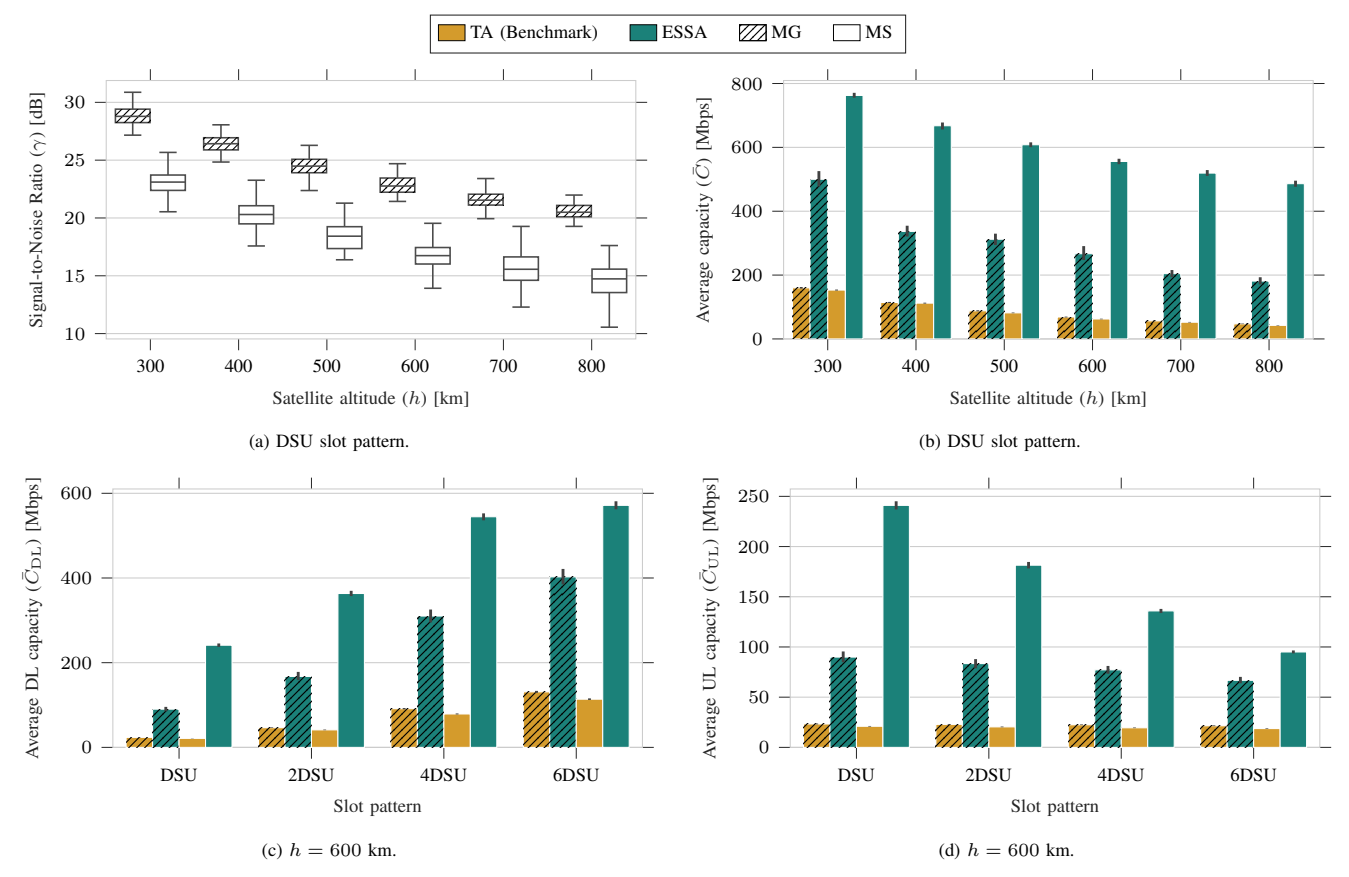
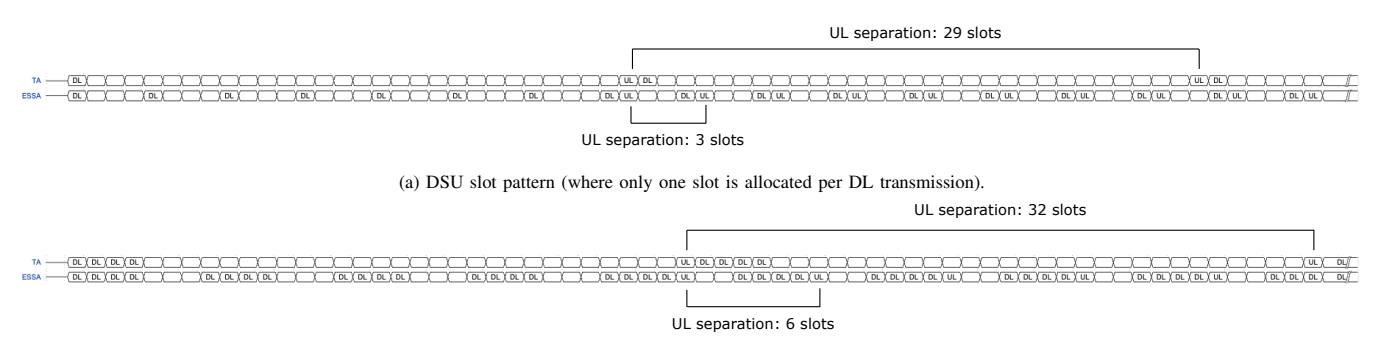


Fig. 4: SNR (γ) and throughput (\bar{C}) of the selected UEs vs. h and the slot pattern.



(b) 4DSU slot pattern (where four slots are scheduled for each DL transmission).

Fig. 5: Example of a slot pattern for a direct-to-satellite connection at h=500 km and $\alpha_{min}=80^{\circ}$. We compare TA vs. ESSA.

slots during guard periods, even if fewer bits per slot are transmitted, which eventually improves resource utilization.

Slot pattern: We now analyze the effect of the slot pattern. In particular, we consider the case in which a DL transmission requires more than one DL slot to be completed, e.g., to satisfy more aggressive traffic requests. The notation XDSU is used to indicate that X consecutive slots are consumed for each DL transmission. As expected, increasing the number of slots dedicated to DL transmissions improves the DL capacity. Considering MG-TA, in Fig. 4c we see that $\bar{C}_{\rm DL}$ increases from approximately 25 Mbps with DSU (where only one slot is allocated per DL transmission) to nearly

130 Mbps with 6DSU (where six slots are scheduled for each DL transmission).

These results also confirm that MS-ESSA outperforms MG-TA. As shown in Fig. 4c, the average DL capacity for TA is up to 130 Mbps with 6DSU, vs. around 570 Mbps for ESSA in the same configuration, i.e., more than 4 times higher. However, in MS-ESSA the use of more DL slots per transmission comes at a significant cost in terms of UL capacity. In Fig. 4d we see that, while in MG-TA $\bar{C}_{\rm UL}$ is almost constant as the number of DL slots increases, in MS-ESSA it drops from around 240 Mbps with DSU to only 95 Mbps with 6DSU. In fact, in MG-TA the frame structure is

sparse due to guard periods, so new DL slots can be allocated by simply shifting UL slots accordingly. In contrast, in MS-ESSA transmissions are scheduled also during guard periods, provided that the condition in Lemma 1 is satisfied, leaving limited flexibility for allocating new DL slots, at the expense of UL slots. In Fig. 5 we compare DSU vs. 4DSU for a direct-to-satellite connection at $h=500~{\rm km}$ and $\alpha_{min}=80^{\circ}$. In this example, the guard period is constant and equal to 29 slots in TA, so UL slots are separated by 29 slots in DSU, vs. $29+(4-1)=32~{\rm in}$ 4DSU. The UL overhead therefore increases by as little as 10% in 4DSU. In ESSA, instead, UL slots are separated by 3 slots in DSU, vs. 6 in 4DSU, so the UL overhead is around 50%.

It is clear that ESSA introduces some bias in the scheduling of DL and UL transmissions, where the latter are sacrificed in favor of the former. As part of our future work, we will improve the design of ESSA to incorporate additional fairness in the allocation of UL and DL slots.

V. CONCLUSIONS AND FUTURE WORKS

The design of advanced TDD schemes can facilitate the integration of TNs and NTNs, ultimately enabling seamless switching between satellite and terrestrial connectivity in uncovered areas or in case of emergency. In this work we proposed an enhanced slot allocation mechanism for TDD NTN called ESSA. The goal is to mitigate the impact of the long propagation delays experienced in satellite networks by allocating additional transmission slots that do not cause interference during guard periods. Moreover, we proposed two scheduling methods to select the optimal UEs that should transmit in TDD to maximize the network capacity. We showed that ESSA can reduce the overhead in DL compared to a baseline solution that simply implements TA to avoid interference, despite some degradation of the UL capacity.

In this paper, the assumption was to design NTNs that operate in TDD like TNs, as promoted in 3GPP NTN Release 17. In our future research, we will also focus on the seamless integration between NTN FDD and TN TDD systems, so as to reduce the complexity of NTN transmissions.

ACKNOWLEDGMENTS

This work was supported by the European Commission through the European Union's Horizon Europe Research and Innovation Programme under the Marie Skłodowska-Curie-SE, Grant Agreement No. 101129618, UNITE. This research was also partially supported by the European Union under the Italian National Recovery and Resilience Plan (NRRP) of NextGenerationEU, partnership on "Telecommunications of the Future" (PE0000001 - program "RESTART").

REFERENCES

[1] A. Chaoub, M. Giordani, B. Lall, V. Bhatia, A. Kliks, L. Mendes, K. Rabie, H. Saarnisaari, A. Singhal, N. Zhang, S. Dixit, and M. Zorzi, "6G for Bridging the Digital Divide: Wireless Connectivity to Remote Areas," *IEEE Wireless Commun.*, pp. 160–168, Jul. 2021.

- [2] H. Shahid, C. Amatetti, R. Campana, S. Tong, D. Panaitopol, A. Vanelli-Coralli, A. Mohamed, C. Zhang, E. Khalifa, E. Medeiros, E. Recayte, F. Ghasemifard, J. Lianghai, J. Bucheli, M. Caus, M. Gurelli, M. A. Vazquez, M. Shaat, N. Borios, P.-E. Eriksson, S. Euler, Z. Li, and X. Fu, "Emerging advancements in 6G NTN radio access technologies: an overview," in *Joint European Conference on Networks and Communications & 6G Summit (EuCNC/6G Summit)*, 2024.
- [3] G. Araniti, A. Iera, S. Pizzi, and F. Rinaldi, "Toward 6G Non-Terrestrial Networks," *IEEE Network*, vol. 36, no. 1, pp. 113–120, Jan./Feb. 2022.
- [4] 3GPP, "Study on New Radio (NR) to support non terrestrial networks (Release 15)," *TR* 38.811, 2018.
- [5] —, "Solutions for NR to support Non-Terrestrial Networks (NTN) (Release 16)," TR 38.821, 2020.
- [6] 3GPP, "Solutions for NR to support Non-Terrestrial Networks (NTN) (Release 17)," Work Item RP-221169, 2022.
- [7] M. Giordani and M. Zorzi, "Non-Terrestrial Networks in the 6G Era: Challenges and Opportunities," *IEEE Network*, vol. 35, no. 2, pp. 244–251, Dec. 2021.
- [8] M. El Jaafari, N. Chuberre, S. Anjuere, and L. Combelles, "Introduction to the 3GPP-defined NTN standard: A comprehensive view on the 3GPP work on NTN," *International Journal of Satellite Communications and Networking*, vol. 41, no. 3, pp. 220–238, Feb. 2023.
- [9] Z. Han, C. Xu, K. Liu, L. Yu, G. Zhao, and S. Yu, "A novel mobile core network architecture for satellite-terrestrial integrated network," in *IEEE Global Communications Conference (GLOBECOM)*, 2021.
- [10] D. Peng, D. He, Y. Li, and Z. Wang, "Integrating terrestrial and satellite multibeam systems toward 6G: techniques and challenges for interference mitigation," *IEEE Wireless Communications*, vol. 29, no. 1, pp. 24–31, Feb. 2022.
- [11] H.-W. Lee, A. Medles, V. Jie, D. Lin, X. Zhu, I.-K. Fu, and H.-Y. Wei, "Reverse spectrum allocation for spectrum sharing between TN and NTN," in *IEEE Conference on Standards for Communications and Networking (CSCN)*, 2021.
- [12] H.-W. Lee, C.-C. Chen, C.-I. S. Liao, A. Medles, D. Lin, I.-K. Fu, and H.-Y. Wei, "Interference mitigation for reverse spectrum sharing in B5G/6G satellite-terrestrial networks," *IEEE Transactions on Vehicular Technology*, vol. 73, no. 3, pp. 4247–4263, Mar. 2024.
- [13] X. Zhu, C. Jiang, L. Kuang, N. Ge, S. Guo, and J. Lu, "Cooperative transmission in integrated terrestrial-satellite networks," *IEEE Network*, vol. 33, no. 3, pp. 204–210, May/Jun. 2019.
- [14] 3GPP, "Non-terrestrial networks (NTN) related RF and co-existence aspects (Release 17)," TR 38.863, 2023.
- [15] _____, "NR and NG-RAN Overall Description (Release 15)," TS 38.300, 2018.
- [16] P. W. C. Chan, E. S. Lo, R. R. Wang, E. K. S. Au, V. K. N. Lau, R. S. Cheng, W. H. Mow, R. D. Murch, and K. B. Letaief, "The evolution path of 4G networks: FDD or TDD?" *IEEE Communications Magazine*, vol. 44, no. 12, pp. 42–50, Dec. 2006.
- [17] A. Traspadini, M. Giordani, G. Giambene, T. De Cola, and M. Zorzi, "On the energy consumption of UAV edge computing in Non-Terrestrial Networks," in 57th Asilomar Conference on Signals, Systems, and Computers, 2023.
- [18] M. Sandri, M. Pagin, M. Giordani, and M. Zorzi, "Implementation of a channel model for non-terrestrial networks in ns-3," in *Proceedings of* the 2023 Workshop on ns-3, 2023.
- [19] D. Wang, M. Giordani, M.-S. Alouini, and M. Zorzi, "The Potential of Multi-Layered Hierarchical Non-Terrestrial Networks for 6G: A Comparative Analysis Among Networking Architectures," *IEEE Vehicular Technolology Magazine*, vol. 16, no. 3, pp. 99–107, Sep. 2021.
- [20] 3GPP, "NR Physical layer procedures for control (Release 15)," TS 38.213, 2018.
- [21] —, "NR Requirements for support of radio resource management (Release 15)," *TS 38.133*, 2018.
- [22] M. M. Saad, M. A. Tariq, M. T. R. Khan, and D. Kim, "Non-Terrestrial Networks: An Overview of 3GPP Release 17 & 18," *IEEE Internet of Things Magazine*, vol. 7, no. 1, pp. 20–26, Jan. 2024.
- [23] M. Giordani and M. Zorzi, "Satellite Communication at Millimeter Waves: a Key Enabler of the 6G Era," *IEEE International Conference* on Computing, Networking and Communications (ICNC), 2020.
- [24] N. Pachler, I. del Portillo, E. F. Crawley, and B. G. Cameron, "An Updated Comparison of Four Low Earth Orbit Satellite Constellation Systems to Provide Global Broadband," in *IEEE International Confer*ence on Communications Workshops (ICC Workshops), 2021.